

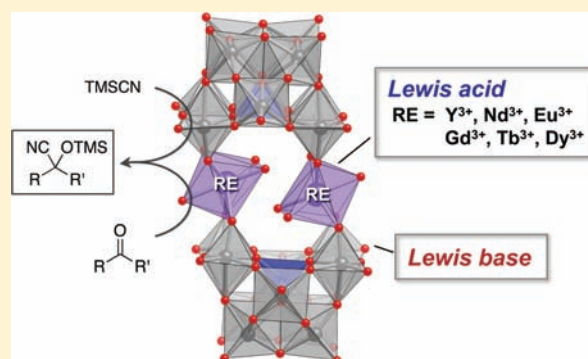
Strategic Design and Refinement of Lewis Acid–Base Catalysis by Rare-Earth-Metal-Containing Polyoxometalates

Kosuke Suzuki, Midori Sugawa, Yuji Kikukawa, Keigo Kamata, Kazuya Yamaguchi, and Noritaka Mizuno*

Department of Applied Chemistry, School of Engineering, The University of Tokyo, 7-3-1 Hongo, Bunkyo-ku, Tokyo 113-8656, Japan

Supporting Information

ABSTRACT: Efficient polyoxometalate (POM)-based Lewis acid–base catalysts of the rare-earth-metal-containing POMs (TBA₆RE-POM, RE = Y³⁺, Nd³⁺, Eu³⁺, Gd³⁺, Tb³⁺, or Dy³⁺) were designed and synthesized by reactions of TBA₄H₄[γ -SiW₁₀O₃₆] (TBA = tetra-*n*-butylammonium) with RE(acac)₃ (acac = acetylacetonato). TBA₆RE-POM consisted of two silicotungstate units pillared by two rare-earth-metal cations. Nucleophilic oxygen-enriched surfaces of negatively charged POMs and the incorporated rare-earth-metal cations could work as Lewis bases and Lewis acids, respectively. Consequently, cyanosilylation of carbonyl compounds with trimethylsilyl cyanide ((TMS)CN) was efficiently promoted in the presence of the rare-earth-metal-containing POMs via the simultaneous activation of coupling partners on the same POM molecules. POMs with larger metal cations showed higher catalytic activities for cyanosilylation because of the higher activation ability of C=O bonds (higher Lewis acidities) and sterically less hindered Lewis acid sites. Among the POM catalysts examined, the neodymium-containing POM showed remarkable catalytic performance for cyanosilylation of various kinds of structurally diverse ketones and aldehydes, giving the corresponding cyanohydrin trimethylsilyl ethers in high yields (13 substrates, 94–99%). In particular, the turnover frequency (714 000 h⁻¹) and the turnover number (23 800) for the cyanosilylation of *n*-hexanal were of the highest level among those of previously reported catalysts.



INTRODUCTION

Polyoxometalates (POMs) are a class of anionic oxoclusters of early transition metals in their highest oxidation states and exhibit a large structural versatility in their sizes, shapes, and numbers of constituent elements.¹ Because of their structural diversities as well as their readily tunable chemical and physical properties, e.g., redox potentials, acidities, charges, electron-transfer properties, and solubilities, they are of increasing interest in potential applications in a wide range of fields including catalysis, medicine, and multifunctional materials. In addition, lacunary POMs can be regarded as oxygen-donor multidentate inorganic macroligands, and the metal substitution into the lacunary POMs is one of the most promising approaches to tune up the chemical and physical properties and to create catalytically active sites at atomic levels.^{2,3} With regard to the catalytic applications, POMs have generally been utilized as Brønsted acid and oxidation catalysts,¹ while their use as Lewis acid catalysts is very rare.⁴ Although hafnium-, zirconium-, and aluminum-containing POMs such as [α -Hf(OH)PW₁₁O₃₉]⁴⁻,^{4a} [M₄O(OH)₆(SiW₁₀O₃₆)₂]⁸⁻ (M = Zr⁴⁺ or Hf⁴⁺),^{4b} and [{Al(OH₂)₂(OH)₂SiW₁₀O₃₆}]^{4-4c} have been reported to act as Lewis acid catalysts for several functional group transformations, the introduced metal cations, i.e., Al³⁺ (ionic radius, 0.68 Å), Zr⁴⁺ (0.86 Å), and Hf⁴⁺ (0.85 Å), are small and deeply incorporated into the lacunary sites of

POM frameworks, resulting in their low catalytic activities and/or limited applications due to the steric hindrance around the active sites.⁴

Among the multitude of POM motifs, rare-earth-metal (RE)-containing POMs offer particularly interesting features.^{5,6} Because of relatively larger ionic radii of RE cations (typically 1.1–1.3 Å), their full incorporation within lacunary sites to form “in-pocket” structures can be prevented. Additionally, high coordination numbers (typically 6–12) with flexible coordination geometries of RE cations can leave residual (open) coordination sites, which would act as effective Lewis acids for activation of substrates.⁷ For example, several RE-containing POMs [α -RE(H₂O)₄P₂W₁₇O₆₁]⁶⁻ and [α -RE(H₂O)-PW₁₁O₃₉]⁴⁻ (RE = Y³⁺, La³⁺, Eu³⁺, Sm³⁺, or Yb³⁺) have been reported to act as efficient Lewis acid catalysts for aldol and imino Diels–Alder reactions.⁷

In addition, other important features of POMs are their bare nucleophilic surfaces composed of the peripheral oxygen atoms of M–O–M and M=O species (M = W, Mo, and so on). The nucleophilic surfaces with large negative charges might act as

Received: April 23, 2012

Revised: May 24, 2012

Accepted: May 25, 2012

Published: June 6, 2012

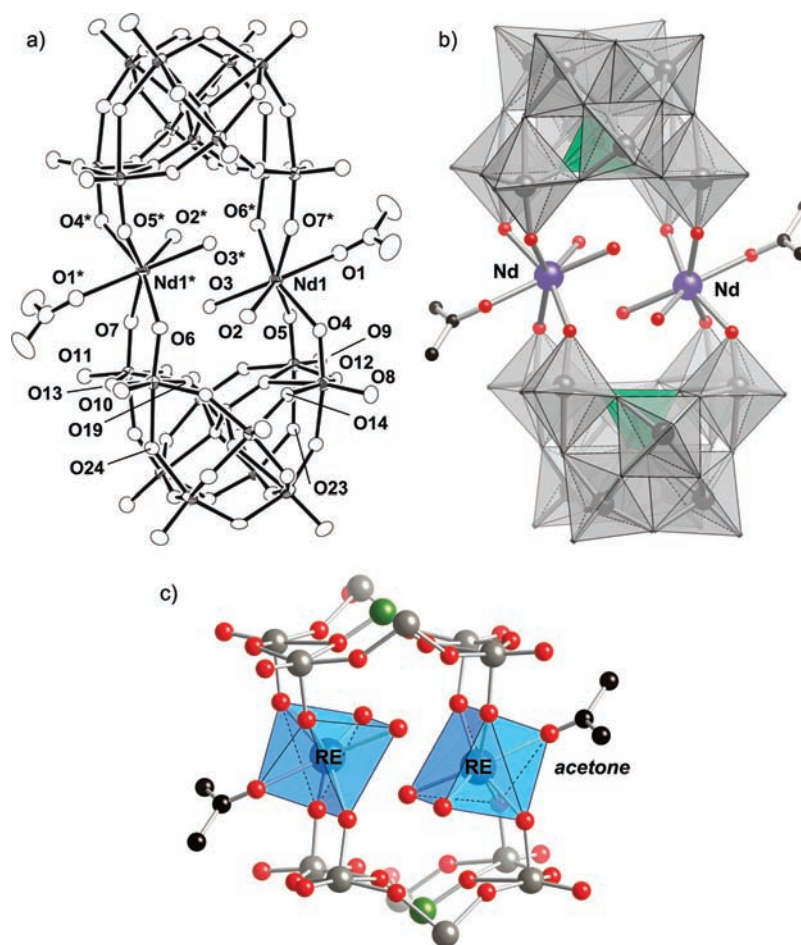


Figure 1. (a) ORTEP representation with thermal ellipsoids drawn at the 50% probability level, (b) polyhedral and ball-and-stick representation of $\text{TBA}_6\text{Nd-POM}$ (the structures of $\text{TBA}_6\text{Y-POM}$, $\text{TBA}_6\text{Eu-POM}$, $\text{TBA}_6\text{Gd-POM}$, $\text{TBA}_6\text{Tb-POM}$, and $\text{TBA}_6\text{Dy-POM}$ are intrinsically identical to that of $\text{TBA}_6\text{Nd-POM}$; see Figure S1), and (c) ball-and-stick and polyhedral representation around $\{\text{RE}(\text{H}_2\text{O})_2(\text{acetone})\}_2$ cores in $\text{TBA}_6\text{RE-POM}$ (RE, blue; W, gray; O, red; C, black; Si, green; the distorted monocapped trigonal prismatic cores around RE cations are shown as transparent blue polyhedra).

Lewis bases and/or stabilizers of cationic reaction intermediates.^{1,8,9} Therefore, we envision that two or more different kinds of substrates would simultaneously be activated by combination of RE Lewis acids and POM Lewis base.

Very recently, we have reported that an yttrium-containing silicotungstate dimer, $[\{\text{Y}(\text{H}_2\text{O})_2\}_2(\gamma\text{-SiW}_{10}\text{O}_{36})_2]^{10-}$, shows remarkable catalytic performance for cyanosilylation of ketones and aldehydes with trimethylsilyl cyanide ((TMS)CN).¹⁰ One of the most important findings is an action of the yttrium-containing POM as a Lewis acid–base catalyst; both carbonyl compounds and (TMS)CN can be activated by the Lewis acid (yttrium cations) and the Lewis base (surface oxygen atoms of the POM), respectively, resulting in coexistence of activated coupling partners on the same POM molecules. Though cyanosilylation can efficiently be promoted by the yttrium-containing POM, there is still room for improvement of the catalytic performance. The rate-limiting step of the cyanosilylation is the nucleophilic attack of CN^- species to a carbonyl compound, and the steric effect around the yttrium cations is not still negligible.¹⁰

Our strategy to design improved Lewis acid–base catalysts is introduction of RE cations with large ionic radii (as Lewis acid sites) into lacunary POMs with large negative charges (as Lewis base sites). Herein, we have successfully synthesized a series of

isostructural γ -Keggin silicotungstate dimers with RE cations, $[\{\text{RE}(\text{H}_2\text{O})_2(\text{acetone})\}_2(\gamma\text{-SiW}_{10}\text{O}_{36})_2]^{10-}$ (RE = Y^{3+} , Nd^{3+} , Eu^{3+} , Gd^{3+} , Tb^{3+} , or Dy^{3+} ; Figures 1 and S1 of the Supporting Information). As we expected, the catalytic activities of the resulting POMs increased with an increase in the ionic radii of the RE cations, and the neodymium-containing POM (with the largest ionic radius) showed the best results. In this paper, we report the synthesis and structural characterization of the RE-containing POMs and their catalytic properties for cyanosilylation. In addition, the scope of cyanosilylation with the most active neodymium-containing POM is described.

RESULTS AND DISCUSSION

Synthesis and Structural Characterization of RE-Containing POMs. Six kinds of tetra-*n*-butylammonium (TBA) salts of the RE-containing POMs with the formulas of $\text{TBA}_6\text{H}_4[\{\text{RE}(\text{H}_2\text{O})_2(\text{acetone})\}_2(\gamma\text{-SiW}_{10}\text{O}_{36})_2] \cdot n(\text{acetone}) \cdot 2\text{H}_2\text{O}$ ($n = 0$ or 1 ; $\text{TBA}_6\text{RE-POM}$; RE = Y^{3+} , Nd^{3+} , Eu^{3+} , Gd^{3+} , Tb^{3+} , or Dy^{3+}) were synthesized by reactions of $\text{TBA}_4\text{H}_4[\gamma\text{-SiW}_{10}\text{O}_{36}]$ with 1 equiv of $\text{RE}(\text{acac})_3$ (acac = acetylacetonato) with respect to $\text{TBA}_4\text{H}_4[\gamma\text{-SiW}_{10}\text{O}_{36}]$ in acetone, followed by addition of 1 equiv of HNO_3 . After 15 min, the RE-containing POMs were obtained in 71–85% yields as white precipitates (see the Experimental Section). The positive-ion cold-spray

ionization mass spectra (CSI-MS) of the products showed sets of signals due to TBA₆RE-POM (Figure S2 of the Supporting Information). For example, two signal sets centered at *m/z* 3559 and 6874 assignable to [TBA₆H₄Nd₂(SiW₁₀O₃₆)₂]²⁺ and [TBA₇H₄Nd₂(SiW₁₀O₃₆)₂]⁺, respectively, were observed for the neodymium-containing POM TBA₆Nd-POM (Figure 2).

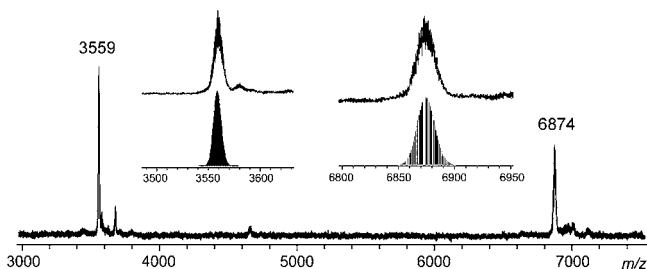


Figure 2. Positive-ion CSI-MS spectra of TBA₆Nd-POM in acetone. Insets: spectra in the range of *m/z* 3490–3640 and 6800–6950 and simulated patterns for [TBA₆H₄Nd₂(SiW₁₀O₃₆)₂]²⁺ (*m/z* 3559) and [TBA₇H₄Nd₂(SiW₁₀O₃₆)₂]⁺ (*m/z* 6874).

These CSI-MS indicate the formation of –10-charged POMs composed of two [SiW₁₀O₃₆]⁸⁻ units and two RE cations and that these POMs were stable in their solution states. Single crystals of all TBA₆RE-POM suitable for X-ray crystallographic analyses were successfully obtained by recrystallization in a mixed solvent of acetonitrile and acetone (1:4, v/v), and their structures were determined. The structure of the anion part of TBA₆Nd-POM is represented in Figure 1 as a typical example (the structures of all TBA₆RE-POM are represented in Figure S1). The crystallographic data and the selected bond lengths and angles of TBA₆RE-POM are summarized in Tables 1 and 2, respectively. As shown in Figure 1, the anion part of TBA₆Nd-POM consisted of a dimer of [γ-SiW₁₀O₃₆]⁸⁻ units pillared by two neodymium cations and possessed the slightly distorted C_{2h} symmetry. The molecular structures of RE-containing POMs TBA₆RE-POM were essentially isomorphous (Figures S1 and S3 of the Supporting Information). To date, several RE-

containing POMs have been reported:^{5,6} for example, monometal-substituted POMs, [α₁-RE(H₂O)₄P₂W₁₇O₆₁]⁶⁻ and [α-RE(H₂O)PW₁₁O₃₉]⁴⁻ (RE = Y³⁺, La³⁺, Eu³⁺, Sm³⁺, or Yb³⁺); sandwich-type POMs, [Y(W₅O₁₈)₂]⁹⁻, [RE(α-SiW₁₁O₃₉)₂]¹³⁻ (RE = Nd³⁺, Pr³⁺, or Ce³⁺), [Yb₆(μ₆-O)(μ₃-OH)₆(H₂O)₆](α-P₂W₁₅O₅₆)¹⁴⁻, and [Y(OH)₂(CO₃)(A-α-PW₉O₃₄)₂]¹¹⁻; multinuclear RE clusters surrounded by POMs, [As₁₂Ce₁₆(H₂O)₃₆W₁₄₈O₅₂₄]⁷⁶⁻, [Gd₈As₁₂-W₁₂₄O₄₃₂(H₂O)₃₆]⁶⁰⁻, and [KC₇Ge₂₄W₁₂₀O₄₅₆(OH)₁₂(H₂O)₆₄]⁵²⁻. To the best of our knowledge, there have been no reports on RE-containing POMs with the γ-Keggin framework.

Elemental analyses showed the existence of six TBA cations per anion and the RE:Si:W ratios of 2:2:20, which are in good agreement with the crystallographic and CSI-MS data. The bond valence sum (BVS)¹¹ values of RE cations (yttrium, 3.11; neodymium, 3.04; europium, 2.81; gadolinium, 2.98; terbium, 2.94; dysprosium, 2.99) in TBA₆RE-POM indicate that all valences are +3. The BVS values of tungsten (5.84–6.15) and silicon (3.80–3.92) in TBA₆RE-POM indicate that the respective valences are +6 and +4. The oxygen atoms O2 and O3 coordinating to RE cations were aqua ligands (water molecules) according to their BVS values (0.32–0.36 for O2 and 0.39–0.47 for O3). The lower BVS values of O23 (1.10–1.13) and O24 (1.13–1.15) in the frameworks of the [γ-SiW₁₀O₃₆]⁸⁻ units suggest protonation of these oxygen atoms. From the data of the above-mentioned characterizations and thermogravimetric analyses, the formulas of these POMs are TBA₆H₄[{RE(H₂O)₂(acetone)}₂{γ-SiW₁₀O₃₆}]₂·n(acetone)·2H₂O (*n* = 0 or 1). The formation of these POMs can be expressed by the following:

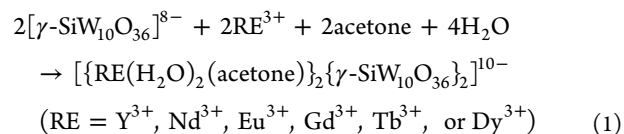


Table 1. Crystal Data and Structure Refinement Parameters for TBA₆RE-POM

	TBA ₆ Y-POM	TBA ₆ Nd-POM	TBA ₆ Eu-POM	TBA ₆ Gd-POM	TBA ₆ Tb-POM	TBA ₆ Dy-POM
molecular formula	C ₁₁₂ Nd ₈ O ₈₀ Si ₂ W ₂₀ Y ₂	C ₁₁₂ Nd ₂ Nd ₈ O ₈₀ Si ₂ W ₂₀	C ₁₁₂ Eu ₂ Nd ₈ O ₈₀ Si ₂ W ₂₀	C ₁₁₂ Gd ₂ Nd ₈ O ₈₀ Si ₂ W ₂₀	C ₁₁₂ Nd ₈ O ₈₀ Si ₂ Tb ₂ W ₂₀	C ₁₁₂ Dy ₂ Nd ₈ O ₈₀ Si ₂ W ₂₀
fw (g mol ⁻¹)	6648.2	6758.86	6774.30	6784.88	6788.22	6795.38
cryst syst	orthorhombic	orthorhombic	orthorhombic	orthorhombic	orthorhombic	orthorhombic
space group	<i>Pbca</i> (No. 61)	<i>Pbca</i> (No. 61)	<i>Pbca</i> (No. 61)	<i>Pbca</i> (No. 61)	<i>Pbca</i> (No. 61)	<i>Pbca</i> (No. 61)
<i>a</i> (Å)	24.22340(10)	25.7060(2)	25.69050(10)	25.6711(2)	25.66720(10)	25.65119(10)
<i>b</i> (Å)	28.79530(10)	24.5296(2)	24.41610(10)	24.3722(2)	24.32180(10)	24.25900(10)
<i>c</i> (Å)	25.64680(10)	28.4474(2)	28.6190(2)	28.6457(2)	28.7271(2)	28.80180(10)
α (deg)	90	90	90	90	90	90
β (deg)	90	90	90	90	90	90
γ (deg)	90	90	90	90	90	90
vol (Å ³)	17889.16(12)	17937.7(2)	17951.61(16)	17922.5(2)	17933.54(16)	17922.56(12)
<i>Z</i>	4	4	4	4	4	4
temp (K)	153(2)	153(2)	153(2)	153(2)	153(2)	153(2)
ρ _{calcd} (g cm ⁻³)	2.468	2.503	2.507	2.515	2.514	2.519
GOF	1.099	1.018	1.003	1.076	1.019	1.056
R ₁ ^a [I > 2σ(I)]	0.0402	0.0486	0.0339	0.0451	0.0408	0.0343
R _{w2} ^a	0.1393	0.1087	0.1042	0.1286	0.1081	0.1083

$$^a R_1 = \sum |F_o| - |F_c| / \sum |F_o|. R_{w2} = \{ \sum [w(F_o^2 - F_c^2)] / \sum [w(F_o^2)] \}^{1/2}.$$

Table 2. Selected Bond Lengths (Å) and Angles (deg) in TBA₆RE-POM

	TBA ₆ Y-POM	TBA ₆ Nd-POM	TBA ₆ Eu-POM	TBA ₆ Gd-POM	TBA ₆ Tb-POM	TBA ₆ Dy-POM
Bond Lengths						
RE1–O(W) _{av}	2.281	2.372	2.332	2.323	2.306	2.295
(O4...O6*, O5...O7*) _{av}	4.446	4.607	4.531	4.512	4.484	4.468
RE1–O1	2.383(6)	2.500(8)	2.457(5)	2.438(6)	2.425(6)	2.409(5)
RE1–O2	2.393(6)	2.483(7)	2.441(5)	2.425(6)	2.418(6)	2.405(5)
RE1–O3	2.367(6)	2.507(7)	2.459(5)	2.433(6)	2.426(6)	2.400(5)
RE1...RE1*	4.5252(9)	4.4828(5)	4.4583(4)	4.4503(4)	4.4615(5)	4.4877(4)
O2...O3*	2.763(6)	2.802(9)	2.788(5)	2.788(6)	2.767(6)	2.752(6)
O2...O6	2.864(8)	2.91(1)	2.894(7)	2.867(8)	2.859(9)	2.857(7)
O3...O7	2.753(8)	2.75(1)	2.746(7)	2.756(8)	2.741(8)	2.749(7)
O2...O14	2.854(8)	2.86(1)	2.856(7)	2.848(8)	2.838(9)	2.846(7)
O3...O19	2.707(7)	2.719(9)	2.695(7)	2.686(7)	2.695(7)	2.701(7)
Bond Angles						
O1–RE1–O2	140.9(2)	140.4(3)	140.20(19)	140.6(2)	140.6(2)	140.91(19)
O2–RE1–O3	72.9(2)	73.8(2)	73.83(17)	73.3(2)	73.4(2)	73.20(18)

Each RE cation (RE1) in TBA₆RE-POM was seven-coordinate to oxygen atoms of one outward acetone (O1), two inward aqua ligands (O2 and O3), and four terminal oxygen atoms of two [γ-SiW₁₀O₃₆]⁸⁻ units (O5, O4, O6*, and O7*). The overall coordination geometries around the RE cations within these anions were best described as a distorted monocapped trigonal prism (Figure 1). This coordination geometry is often observed in coordination compounds of RE¹² and RE-containing POMs.^{5n-p} Each RE cation was located “out-of-pocket” without the direct interaction with the central SiO₄ tetrahedron, which is more desirable as Lewis acid centers in comparison with “in-pocket” structures from the steric viewpoint.^{4b} The distances between oxygen atoms of aqua ligands (O2 and O3) on RE cations and the neighbor oxygen atoms of the [γ-SiW₁₀O₃₆]⁸⁻ frameworks (O2...O3*, O2...O6, O3...O7, O2...O14, and O3...O19) were within the range of hydrogen-bonding distances (2.69–2.91 Å; Table 2).¹³ Thus, the hydrogen-bonding networks between these oxygen atoms likely stabilize the unique configuration around RE cations and the slipped structures of the dimer of [γ-SiW₁₀O₃₆]⁸⁻ units. The angles of O1–RE1–O2 and O2–RE1–O3 were 140.2–140.9 and 72.9–73.8° (Table 2), respectively.

The average bond lengths between the RE cations and the oxygen atoms of [γ-SiW₁₀O₃₆]⁸⁻ units (RE1–O(W)_{av}) increased in the order of TBA₆Y-POM (2.281 Å) < TBA₆Dy-POM (2.295 Å) < TBA₆Tb-POM (2.306 Å) < TBA₆Gd-POM (2.323 Å) < TBA₆Eu-POM (2.332 Å) < TBA₆Nd-POM (2.372 Å) (Table 2) with an increase in the ionic radii (Y³⁺ (1.16 Å) < Dy³⁺ (1.17 Å) < Tb³⁺ (1.18 Å) < Gd³⁺ (1.19 Å) < Eu³⁺ (1.21 Å) < Nd³⁺ (1.25 Å) for eight coordination),¹⁴ showing that interactions between the RE cations and the two sandwiching [γ-SiW₁₀O₃₆]⁸⁻ POMs weaken with an increase in ionic radii of the RE cations. In addition, distances between oxygen atoms surrounding the RE atoms (O4...O6* and O5...O7*), which reflect the sizes of spaces between the two sandwiching [γ-SiW₁₀O₃₆]⁸⁻ POMs, depended on ionic radii of RE cations, and the average distances of O4...O6* and O5...O7* increased with an increase in ionic radii of the RE cations (Table 2). These results suggest that the steric crowding around Lewis acid centers decreases with an increase in ionic radii of RE cations.

Most importantly, acetone molecules were coordinated to the RE cations in TBA₆RE-POM, suggesting that these sites act as Lewis acid centers to activate carbonyl compounds. The stretching vibration band of the C=O bond ($\nu(\text{C}=\text{O})$) of

noncoordinated acetone was observed at 1715 cm⁻¹, and those of the coordinated acetone molecules on TBA₆RE-POM appeared at lower wavenumbers in the order of TBA₆Y-POM (1696 cm⁻¹) < TBA₆Dy-POM (1694 cm⁻¹) < TBA₆Tb-POM (1692 cm⁻¹) < TBA₆Gd-POM (1691 cm⁻¹) < TBA₆Eu-POM (1688 cm⁻¹) < TBA₆Nd-POM (1685 cm⁻¹) (Table 3 and

Table 3. Cyanosilylation of **1a** with TBA₆RE-POM^a

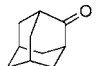
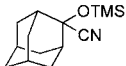
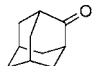
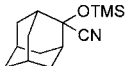
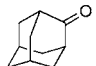
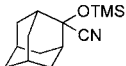
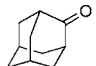
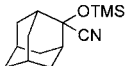
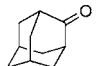
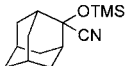
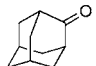
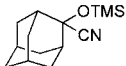
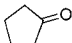
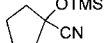
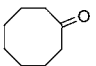
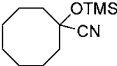
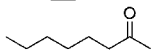
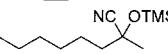
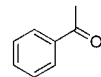
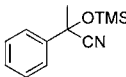
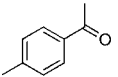
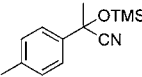
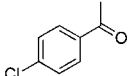
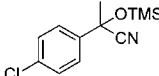
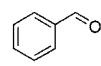
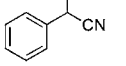
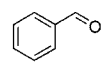
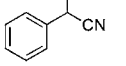
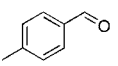
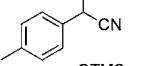
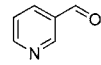
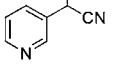
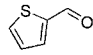
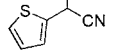
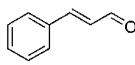
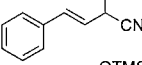
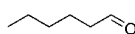
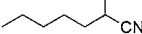
entry	catalyst	yield of 2a (%)	$\nu(\text{C}=\text{O})$ (cm ⁻¹) ^b	ionic radius of RE ³⁺ (Å) ^c
1	TBA ₆ Nd-POM	66	1685	1.25
2	TBA ₆ Eu-POM	53	1688	1.21
3	TBA ₆ Gd-POM	50	1691	1.19
4	TBA ₆ Tb-POM	41	1692	1.18
5	TBA ₆ Dy-POM	29	1694	1.17
6	TBA ₆ Y-POM	41	1696	1.16

^aReaction conditions: catalyst (0.5 mol %), **1a** (0.25 mmol), (TMS)CN (1.5 equiv to **1a**), acetonitrile (2 mL), 30 °C, 30 min. Yields were determined by GC using naphthalene as an internal standard. Selectivities to **2a** were >99% in all cases. ^b $\nu(\text{C}=\text{O})$ of acetone molecules coordinated to RE cations in TBA₆RE-POM (see Figure S4). ^cIonic radius of RE³⁺ for eight coordination.¹⁴

Figure S4 of the Supporting Information).¹⁵ These lower wavenumber shifts show that acetone is electrophilically activated by Lewis acid centers of TBA₆RE-POM and that the neodymium-containing POM possesses the highest C=O bond activation ability (Lewis acidity) among a series of TBA₆RE-POM. The higher C=O activation ability of TBA₆RE-POM with larger RE cations is likely explained by the weaker interaction between RE cations and sandwiching [γ-SiW₁₀O₃₆]⁸⁻ POMs, while Lewis acidities of bare RE cations without coordinating ligands decrease with an increase in the ionic radii.

Cyanosilylation with RE-Containing POMs. Very recently, we have reported that the yttrium-containing γ-Keggin POMs TBA₆Y-POM and TBA₈H₂[{Y(H₂O)₂]₂(γ-SiW₁₀O₃₆)₂·3H₂O (TBA₈Y-POM) show remarkable catalytic activities for cyanosilylation of carbonyl compounds with (TMS)CN.¹⁰ Both carbonyl compounds and (TMS)CN are

Table 4. Cyanosilylation of Ketones and Aldehydes with TMS(CN) Catalyzed by TBA₈Nd-POM^a

entry	substrate	time (min)	product	yield (%)		
1		7		98		
2 ^b		7		98		
3 ^b		7		97		
4 ^b		7		98		
5 ^b		7		96		
6 ^b		7		98		
7		1b	25		2b	97
8		1c	120		2c	96
9		1d	20		2d	95
10		1e	30		2e	97
11		1f	90		2f	96
12		1g	20		2g	96
13 ^c		1h	2		2h	99
14 ^d		10				95
15 ^c		1i	2		2i	98
16 ^c		1j	2		2j	99
17 ^c		1k	2		2k	99
18 ^c		1l	4		2l	94
19 ^c		1m	2		2m	95

^aReaction conditions: TBA₈Nd-POM (0.5 mol %), ketone (0.25 mmol), (TMS)CN (1.5 equiv with respect to ketone), acetonitrile (1.0 mL), 30 °C.

^bThese experiments used a recovered catalyst; first reuse (entry 2), second reuse (entry 3), third reuse (entry 4), fourth reuse (entry 5), and fifth (entry 6).

^cReaction conditions: TBA₈Nd-POM (0.1 mol %), aldehyde (0.5 mmol), (TMS)CN (1.5 equiv.), 1,2-dichloroethane (0.5 mL), 25 °C.

^dReaction conditions: TBA₈Nd-POM (0.004 mol %), aldehyde (1.0 mmol), (TMS)CN (1.5 equiv.), 1,2-dichloroethane (0.5 mL), 25 °C. Yields were determined by GC and/or ¹H NMR using naphthalene as an internal standard.

synergistically activated by the Lewis acidic yttrium centers (electrophilically) and the surface oxygen atoms of POMs (nucleophilically), respectively, on the same POM molecules.¹⁰ In ¹³C NMR spectra, a methyl signal of (TMS)CN (−1.95 ppm) in 1,2-dichloroethane-*d*₄ disappeared upon addition of TBA₄H₄[γ-SiW₁₀O₃₆], and a new signal (1.01 ppm) assignable to a methyl group of trimethylsilanol appeared, indicating that (TMS)CN is activated by [γ-SiW₁₀O₃₆]^{8−} and reacts with water included in solvents and/or TBA₄H₄[γ-SiW₁₀O₃₆]. Additionally, the CSI-MS of the mixture of TBA₄H₄[γ-SiW₁₀O₃₆] with (TMS)CN showed a set of signals assignable to [TBA₅TMS₄SiW₁₀O₃₆]⁺ (Figure S5 of the Supporting Information), indicating that trimethylsilyl (TMS) cations surround POM anions. As above-mentioned, acetone molecules were electrophilically activated on the RE cations. Thus, the coexisting of activated coupling partners on the same POM molecules resulted in the effective promotion of cyanosilylation. Because the rate-limiting step of the yttrium-POMs-catalyzed

cyanosilylation is the nucleophilic attack of CN[−] species to a carbonyl compound,¹⁰ it is expected that the catalysts with higher activation ability for C=O bonds of carbonyl compounds would show higher catalytic activities. As shown by the crystallographic and IR data, increasing the ionic radii of RE cations resulted in improving both (1) the steric hindrance around Lewis acid centers and (2) the C=O bond activation ability (Lewis acidity). Therefore, POMs with larger RE cations would be effective for cyanosilylation.

First, we carried out the cyanosilylation of 2-adamantanone (1a) as a model reaction to investigate the catalytic nature of a series of TBA₆RE-POM. The reaction was carried out with 0.5 mol % of TBA₆RE-POM under the conditions described in Table 3. In the absence of catalysts, no cyanosilylation of 1a proceeded under the present conditions. TBA₆RE-POM effectively catalyzed the cyanosilylation to afford the corresponding cyanohydrin trimethylsilyl ether 2a. As we expected, the catalytic activities of TBA₆RE-POM increased with an

increase in the ionic radii of RE cations in TBA₆RE-POM (Table 3). For example, the yields of **2a** at 30 min were 50 and 66% in the presence of TBA₆Gd-POM and TBA₆Nd-POM, respectively, while 41% in the presence of TBA₆Y-POM. Among TBA₆RE-POM catalysts examined, the neodymium-containing POM TBA₆Nd-POM (with the largest RE cation) showed the highest activity for this reaction.

Scope of the Neodymium-Containing POM-Catalyzed Cyanosilylation. Finally, the scope of the cyanosilylation of various carbonyl compounds by the most active neodymium-containing POM was examined. Because of the very low solubility of TBA₆Nd-POM in organic solvents, e.g., below 0.05 mM in 1,2-dichloroethane, we used TBA₈H₂[{Nd(H₂O)₂}(γ -SiW₁₀O₃₆)₂].3H₂O (TBA₈Nd-POM) which is readily soluble in various organic solvents. From the IR and CSI-MS spectra (Figures S6 and S7 of the Supporting Information), and elemental analysis, the anion structure of TBA₈Nd-POM was identical to that of TBA₆Nd-POM.¹⁶ First, we examined the effect of solvents on the cyanosilylation of **1a**. Among various solvents examined, acetonitrile was the best solvent (Table S1 of the Supporting Information). *N,N*-Dimethylformamide, 1,2-dichloroethane, and tetrahydrofuran also gave high yields of **2a** (Table S1). The catalytic activity of TBA₈Nd-POM in acetonitrile was higher than those of TBA₄H₄[γ -SiW₁₀O₃₆] and Nd(acac)₃, and even higher than that of previously reported TBA₈Y-POM (Scheme S1 of the Supporting Information).¹⁷

In the presence of TBA₈Nd-POM under optimized conditions, various kinds of structurally diverse ketones and aldehydes could react with (TMS)CN to produce the corresponding cyanohydrin trimethylsilyl ethers. No desilylated products were formed in all cases. Sterically less hindered cyclic (**1b**) and linear aliphatic (**1d**) ketones smoothly reacted with (TMS)CN to afford the corresponding products in high yields. The cyanosilylation of sterically more hindered aliphatic cyclic ketones such as 2-adamantanone (**1a**) and cyclooctanone (**1c**) also efficiently proceeded to give the corresponding cyanohydrin trimethylsilyl ethers in high yields, and the catalytic performance of TBA₈Nd-POM for these bulky ketones was in remarkable contrast with the low catalytic activity of TBA₈Y-POM.¹⁰ For example, the cyanosilylation of **1c** with TBA₈Nd-POM almost quantitatively afforded **2c** for 120 min, while that with TBA₈Y-POM required a longer reaction time (240 min) to attain a high yield (90% yield) of **2c**. This is likely because the larger spaces around the neodymium cations result in higher accessibility of bulky ketones to the Lewis acidic sites of POMs (Figure S8 of the Supporting Information). Less reactive acetophenone derivatives (**1e–1g**) were also converted into the corresponding cyanohydrin trimethylsilyl ethers in high yields. TBA₈Nd-POM showed the quite high catalytic performance for cyanosilylation of benzaldehyde derivatives, giving the corresponding products in quantitative yields within 2 min using only 0.1 mol % TBA₈Nd-POM. The present system was also applicable to heteroatom-containing aldehydes such as 3-pyridinecarboxaldehyde (**1j**) and 2-thiophenecarboxaldehyde (**1k**). An α,β -unsaturated aldehyde of *trans*-cinnamaldehyde (**1l**) also selectively gave the corresponding product without formation of the 1,4-addition product. With regard to an aliphatic aldehyde, the amount of the catalyst could be much reduced; the cyanosilylation of *n*-hexanal (**1m**) efficiently proceeded with only “0.004 mol % of TBA₈Nd-POM”, giving **2m** in 95% yield for 2 min. In this case, the turnover frequency (TOF) was 714 000 h⁻¹, and the turnover number (TON)

reached up to 23 800. These TOF and TON values were of the highest level among those of previously reported catalysts including TBA₈Y-POM (Table S2 of the Supporting Information).^{18–20}

The products could easily be isolated in high yields (see the Experimental Section). After the cyanosilylation was completed, TBA₈Nd-POM could be retrieved in almost quantitative yields ($\geq 93\%$ catalyst recovery) by evaporation of the solvent followed by addition of an excess amount of *n*-hexane (see the Experimental Section). The IR spectrum of the retrieved catalyst was identical to that of as-prepared TBA₈Nd-POM (Figure S9 of the Supporting Information), suggesting that the structure of TBA₈Nd-POM was preserved after the cyanosilylation. In addition, the retrieved catalyst could be reused at least five times without an appreciable loss of its high catalytic activity for the cyanosilylation of **1a** (entries 2–6 in Table 4); even for the fifth reuse experiment, 98% yield of **2a** was obtained.

CONCLUSIONS

The RE-containing silicotungstate dimers (TBA₆RE-POM, RE = Y³⁺, Nd³⁺, Eu³⁺, Gd³⁺, Tb³⁺, or Dy³⁺) were synthesized by reactions of TBA₄H₄[γ -SiW₁₀O₃₆] with RE(acac)₃ in acetone, and their structures were successfully determined. The POMs consisted of two [γ -SiW₁₀O₃₆]⁸⁻ units pillared by two RE cations, and acetone was coordinated to each RE cation. Combining the nucleophilic Lewis base surface of POMs with Lewis acid metal centers, these RE-containing POMs could act as Lewis acid–base catalysts and effectively promote cyanosilylation of carbonyl compounds with (TMS)CN. In particular, the catalytic properties could finely be tuned by selection of introduced RE cations; i.e., POMs with larger metal cations showed higher catalytic activities for cyanosilylation because of the higher activation ability of C=O bonds (higher Lewis acidities) and sterically less hindered Lewis acid sites. Among the POM catalysts examined, the neodymium-containing POM TBA₈Nd-POM showed the remarkable catalytic performance and was applicable to cyanosilylation of various kinds of structurally diverse ketones and aldehydes, giving the corresponding cyanohydrin trimethylsilyl ethers in high yields without formation of the desilylated products. The TOF and TON values obtained with TBA₈Nd-POM were of the highest level among those of previously reported catalysts.

EXPERIMENTAL SECTION

General Methods. The GC analyses were performed on Shimadzu GC-2014 with a flame ionization detector (FID) equipped with a TC-5 (internal diameter = 0.25 mm, length = 60 m), TC-1 (internal diameter = 0.32 mm, length = 30 m), or Rxi-5 Sil (internal diameter = 0.25 mm, length = 30 m) capillary column. The GC mass spectra were recorded on Shimadzu GCMS-QP2010 equipped with a InertCap SMS/SIL capillary column at an ionization voltage of 70 eV. The IR spectra were measured on JASCO FT/IR-460 using KBr disks. The liquid-state NMR spectra were recorded on JEOL JNM-EX-270. ¹H (internal standard, TMS) and ¹³C{H} (internal standard, TMS) spectra were measured at 270 and 67.8 MHz, respectively. The CSI-MS were recorded on JEOL JMS-T100CS. The thermogravimetric and differential thermal analyses (TG-DTA) were performed on Rigaku Thermo plus TG 8120. The ICP-AES analyses were performed with Shimadzu ICPS-8100. Metal salts were obtained from Wako, KANTO, Nacalai, or Aldrich (reagent grade), and used as received. TBA₄H₄[γ -SiW₁₀O₃₆].2H₂O (SiW10) was synthesized according to the reported procedures.²¹ Solvents and substrates were obtained from TCI,

Nacalai, Fluka, Acros, or KANTO (reagent grade) and purified prior to use (if necessary).

X-ray Crystallography. The diffraction measurements were made on a Rigaku MicroMax-007 Saturn 724 CCD detector with graphite-monochromated Mo $K\alpha$ radiation ($\lambda = 0.71069 \text{ \AA}$) at -120 or -150 °C. The data were collected and processed using CrystalClear²² for Windows software and HKL2000²³ for Linux software. Neutral scattering factors were obtained from the standard source. In the reduction of data, Lorentz and polarization corrections were made. The structural analyses were performed using CrystalStructure,²⁴ WinGX,²⁵ and Yadokari-XG.²⁶ All structures were solved by SHELXS-97 (direct methods) and refined by SHELXL-97.²⁷ The metal atoms (Si, W, and RE), oxygen atoms in the POM frameworks, and oxygen and carbon atoms of coordinated acetone molecules were refined anisotropically. CCDC-869962 (TBA₆Nd-POM), CCDC-869963 (TBA₆Eu-POM), CCDC-869964 (TBA₆Gd-POM), CCDC-869965 (TBA₆Tb-POM), and CCDC-869966 (TBA₆Dy-POM) contain the supplementary crystallographic data for this paper. These data can be obtained free of charge from The Cambridge Crystallographic Data Centre via www.ccdc.cam.ac.uk/data_request/cif or the Supporting Information.

Synthesis of TBA₆Y-POM. TBA₆Y-POM was synthesized according to the previously reported procedure.¹⁰ To an acetone solution of SiW10 (1.0 g, 0.29 mmol, 20 mL), Y(acac)₃·11H₂O (170 mg, 0.29 mmol, 1 equiv with respect to SiW10), and HNO₃ (1 M, 0.29 mL, 1 equiv. with respect to SiW10) were added, and the resulting solution was stirred for 15 min at room temperature (ca. 20 °C). Then, the white precipitate formed was filtered off, washed with acetone, and air-dried to afford 810 mg of TBA₆Y-POM (85% yield based on SiW10). The colorless crystals of TBA₆Y-POM suitable for the X-ray crystallographic analysis were obtained by recrystallization from a mixed solvent of acetone and acetonitrile (4:1, v/v/v). Elem. Anal. Calcd (%) for C₁₀₅H₂₅₀Si₂N₆O₈₁W₂₀Y₂ (TBA₆H₄[{Y-(H₂O)₂(CH₃COCH₃)₂}(SiW₁₀O₃₆)₂}]·(CH₃COCH₃)₂·2H₂O): C, 18.66; H, 3.78; N, 1.27; Si, 0.83; W, 54.22; Y, 2.62. Found: C, 18.54; H, 3.70; N, 1.24; Si, 0.83; W, 54.04; Y, 2.61. Positive-ion MS (CSI, CH₃CN): m/z 6764 [TBA₆H₄Y₂(SiW₁₀O₃₆)₂]⁺, 3503 [TBA₈H₄Y₂(SiW₁₀O₃₆)₂]²⁺. IR (KBr pellet, cm⁻¹): 1710, 1701, 1697, 1623, 1484, 1466, 1420, 1383, 1363, 1282, 1242, 1222, 1152, 1105, 999, 962, 891, 818, 758, 553, 511, 460, 384, 362, 305.

Synthesis of TBA₆Nd-POM. To an acetone solution of SiW10 (200 mg, 0.0582 mmol, 4 mL), Nd(acac)₃ (25.7 mg, 0.0582 mmol, 1 equiv with respect to SiW10) and HNO₃ (1 M, 0.058 mL, 1 equiv with respect to SiW10) were added, and the resulting solution was stirred for 15 min at room temperature (ca. 20 °C). Then, the white precipitate formed was filtered off, washed with acetone, and air-dried to afford 167 mg of TBA₆Nd-POM (84% yield based on SiW10). The colorless crystals of TBA₆Nd-POM suitable for the X-ray crystallographic analysis were obtained by recrystallization from a mixed solvent of acetone and acetonitrile (4:1, v/v). Elem. Anal. Calcd (%) for C₁₀₂H₂₄₄Si₂N₆O₈₀W₂₀Nd₂ (TBA₆H₄[{Nd-(H₂O)₂(CH₃COCH₃)₂}(SiW₁₀O₃₆)₂}]·2H₂O): C 17.87, H 3.59, N 1.23, Si 0.82, Nd 4.21, W 53.63. Found: C 17.82, H 3.70, N 1.31, Si 0.84, Nd 4.50, W 53.92. Positive-ion MS (CSI, acetone): m/z 6874 [TBA₇H₄Nd₂(SiW₁₀O₃₆)₂]⁺, 3559 [TBA₈H₄Nd₂(SiW₁₀O₃₆)₂]²⁺. IR (KBr pellet, cm⁻¹): 2961, 2933, 2873, 1685, 1627, 1484, 1470, 1382, 1243, 1152, 1105, 998, 962, 874, 757, 554, 461, 381, 361, 311.

Synthesis of TBA₈Nd-POM. To an acetone solution of SiW10 (1.50 g, 0.437 mmol, 30 mL), Nd(acac)₃ (0.193 g, 0.437 mmol, 1 equiv with respect to SiW10) was added, and the resulting solution was stirred for 15 min at room temperature (ca. 20 °C). Then, the pale blue precipitate formed was filtered off, washed with diethyl ether, and air-dried to afford 1.10 g of TBA₈Nd-POM in 70% yield (0.152 mmol). The pale blue crystals of TBA₈Nd-POM were obtained by recrystallization from a mixed solvent of acetone, acetonitrile, and diethyl ether (1:2:1, v/v). Elem. Anal. Calcd (%) for C₁₂₈H₃₀₄Si₂N₈O₇₉Nd₂W₂₀ (TBA₈H₂[Nd₂(SiW₁₀O₃₆)₂]}·7H₂O): C, 21.23; H, 4.23; N, 1.55; Si, 0.78; Nd, 3.98; W, 50.78. Found: C, 21.18; H, 4.37; N, 1.51; Si, 0.80; Nd, 4.03; W, 55.44. Positive-ion MS (CSI, 1,2-dichloroethane): m/z 7357 [TBA₉H₂Nd₂(SiW₁₀O₃₆)₂]⁺,

3 9 2 1 [TBA₁₁HNd₂(SiW₁₀O₃₆)₂]²⁺, 3 8 0 0 [TBA₁₀H₂Nd₂(SiW₁₀O₃₆)₂]²⁺. IR (KBr pellet, cm⁻¹): 2960, 2932, 2872, 1634, 1600, 1517, 1483, 1382, 1263, 1153, 1106, 1066, 996, 953, 871, 751, 554, 461, 360, 309.

Synthesis of TBA₆Eu-POM. TBA₆Eu-POM was synthesized via the same procedure as that for TBA₆Nd-POM except that Eu(acac)₃ was used (colorless crystals, 161 mg, 80% yield based on SiW10). Elem. Anal. Calcd (%) for C₁₀₂H₂₄₄Si₂N₆O₈₀W₂₀Eu₂ (TBA₆H₄[{Eu-(H₂O)₂(CH₃COCH₃)₂}(SiW₁₀O₃₆)₂}]·2H₂O): C, 17.83; H, 3.58; N, 1.22; Si, 0.82; Eu, 4.42; W, 53.50. Found: C, 17.68; H, 3.67; N, 1.19; Si, 0.84; Eu, 4.54; W, 53.69. Positive-ion MS (CSI, CH₃CN): m/z 6888 [TBA₇H₄Eu₂(SiW₁₀O₃₆)₂]⁺, 3687 [TBA₈H₃Eu₂(SiW₁₀O₃₆)₂]²⁺, 3567 [TBA₈H₄Eu₂(SiW₁₀O₃₆)₂]²⁺. IR (KBr pellet, cm⁻¹): 2962, 2932, 2874, 1708, 1688, 1627, 1484, 1470, 1423, 1381, 1360, 1243, 1223, 1151, 1105, 998, 960, 876, 820, 759, 668, 629, 555, 512, 459.

Synthesis of TBA₆Gd-POM. TBA₆Gd-POM was synthesized via the same procedure as that for TBA₆Nd-POM except that Gd(acac)₃ was used (colorless crystals, 162 mg, 81% yield based on SiW10). Elem. Anal. Calcd (%) for C₁₀₅H₂₅₀Si₂N₆O₈₁W₂₀Gd₂ (TBA₆H₄[{Gd-(H₂O)₂(CH₃COCH₃)₂}(SiW₁₀O₃₆)₂}]·(CH₃COCH₃)₂·2H₂O): C, 18.17; H, 3.63; N, 1.21; Si, 0.81; W, 52.98; Gd, 4.53. Found: C, 18.19; H, 3.61; N, 1.30; Si, 0.82; W, 52.67; Gd, 4.71. Positive-ion MS (CSI, acetone): m/z 6900 [TBA₇H₄Gd₂(SiW₁₀O₃₆)₂]⁺, 3572 [TBA₈H₄Gd₂(SiW₁₀O₃₆)₂]²⁺. IR (KBr pellet, cm⁻¹): 2962, 2935, 2874, 1710, 1691, 1625, 1484, 1420, 1382, 1362, 1241, 1221, 1152, 1106, 998, 962, 876, 760, 553, 461.

Synthesis of TBA₆Tb-POM. TBA₆Tb-POM was synthesized via the same procedure as that for TBA₆Nd-POM except that Tb(acac)₃ was used (colorless crystals, 170 mg, 81% yield based on SiW10). Elem. Anal. Calcd (%) for C₁₀₂H₂₄₄Si₂N₆O₈₀W₂₀Tb₂ (TBA₆H₄[{Tb-(H₂O)₂(CH₃COCH₃)₂}(SiW₁₀O₃₆)₂}]·2H₂O): C, 17.79; H, 3.57; N, 1.22; Si, 0.82; W, 53.40; Tb, 4.62. Found: C, 17.96; H, 3.69; N, 1.30; Si, 0.83; W, 53.84; Tb, 4.98. Positive-ion MS (CSI, CH₃CN): m/z 3573 [TBA₈H₄Tb₂(SiW₁₀O₃₆)₂]⁺. IR (KBr pellet, cm⁻¹): 2962, 2937, 2873, 1710, 1692, 1627, 1484, 1468, 1419, 1382, 1361, 1242, 1221, 1151, 1105, 999, 962, 887, 817, 759, 668, 627, 554, 551, 461.

Synthesis of TBA₆Dy-POM. TBA₆Dy-POM was synthesized via the same procedure as that for TBA₆Nd-POM except that Dy(acac)₃ was used (colorless crystals, 143 mg, 71% yield based on SiW10). Elem. Anal. Calcd (%) for C₁₀₂H₂₄₄Si₂N₆O₈₀W₂₀Dy₂ (TBA₆H₄[{Dy-(H₂O)₂(CH₃COCH₃)₂}(SiW₁₀O₃₆)₂}]·2H₂O): C, 17.77; H, 3.57; N, 1.22; Si, 0.82; W, 53.34; Dy, 4.71. Found: C, 17.86; H, 3.71; N, 1.33; Si, 0.83; W, 53.67; Dy, 4.78. Positive-ion MS (CSI, CH₃CN): m/z 3576 [TBA₈H₄Dy₂(SiW₁₀O₃₆)₂]²⁺. IR (KBr pellet, cm⁻¹): 2961, 2932, 2873, 1710, 1693, 1634, 1484, 1466, 1419, 1383, 1361, 1242, 1223, 1151, 1106, 999, 962, 886, 817, 758, 670, 627, 552, 511, 461.

Cyanosilylation. The detailed reaction conditions are shown in the footnotes of the tables. A typical procedure for cyanosilylation of carbonyl compounds is as follows: Into a Pyrex-glass screw cap vial were successively placed TBA₈Nd-POM (0.5 mol %), **1a** (0.25 mmol), and acetonitrile (1.0 mL). A Teflon-coated magnetic stir bar was added, and the reaction was initiated by addition of (TMS)CN (0.375 mmol). The reaction mixture was vigorously stirred (800 rpm) at 30 °C in 1 atm of air. The conversion of **1a** and the product yield were periodically determined by GC analysis. After the reaction was completed (>99% conversion of **1a** for 7 min), acetonitrile was evaporated, followed by addition of *n*-hexane to precipitate the catalyst. The catalyst was removed by filtration (17 mg, 93% catalyst recovery), followed by column chromatography on silica gel (eluent: *n*-hexane), giving the corresponding cyanohydrin trimethylsilyl ether **2a** (0.0598 g, 96% isolated yield). All products (cyanohydrin trimethylsilyl ethers) were confirmed by comparison of their GC retention times, GC-mass spectra, and/or ¹H and ¹³C NMR spectra with those of authentic data. The retrieved catalyst was washed with *n*-hexane (ca. 50 mL), and then air-dried prior to being used for the reuse experiment. The IR spectrum of the retrieved TBA₈Nd-POM was intrinsically identical to that of as-prepared TBA₈Nd-POM (Figure S9). When the cyanosilylation of **1a** was carried out with the retrieved catalyst under the conditions in Table 4, **2a** was obtained in 98% yield.

■ ASSOCIATED CONTENT

■ Supporting Information

Crystallographic data for TBA₆Nd-POM, TBA₆Eu-POM, TBA₆Gd-POM, TBA₆Tb-POM, TBA₆Dy-POM, and TBA₆Y-POM (CIF) and ORTEP representations, CSI-MS and IR spectra, and a structural model (Figures S1–S10), cyanosilylation of **1a** (Scheme S1), and cyanosilylation of **1a**, ketones, and aldehydes (Tables S1 and S2) (pdf). This material is available free of charge via the Internet at <http://pubs.acs.org>.

■ AUTHOR INFORMATION

Corresponding Author

*Tel.: +81-3-5841-7272. Fax: +81-3-5841-7220. E-mail: tmizuno@mail.ecc.u-tokyo.ac.jp.

Notes

The authors declare no competing financial interest.

■ ACKNOWLEDGMENTS

We thank Mr. T. Hirano (The University of Tokyo) for his help with preliminary experiments. This work was supported by a Grant-in-Aid for Scientific Research from the Ministry of Education, Culture, Science, Sports, and Technology of Japan (MEXT) and the Funding Program for World-Leading Innovative R&D on Science and Technology (FIRST Program).

■ REFERENCES

- (1) (a) Hill, C. L.; Prosser-McCartha, C. M. *Coord. Chem. Rev.* **1995**, *143*, 407–455. (b) Okuhara, T.; Mizuno, N.; Misono, M. *Adv. Catal.* **1996**, *41*, 113–252. (c) Neumann, R. *Prog. Inorg. Chem.* **1998**, *47*, 317–370. (d) Thematic issue on polyoxometalates: Hill, C. L. *Chem. Rev.* **1998**, *98*, 1–390. (e) Kozhevnikov, I. V. *Catalysis by Polyoxometalates*; John Wiley & Sons: Chichester, U.K., 2002. (f) Kortz, U.; Müller, A.; Slageren, J.; Schnack, J.; Dalal, N. S.; Dressel, M. *Coord. Chem. Rev.* **2009**, *253*, 2315–2327.
- (2) (a) Putaj, P.; Lefebvre, F. *Coord. Chem. Rev.* **2011**, *255*, 1642–1685. (b) Long, D.-L.; Tsunashima, R.; Cronin, L. *Angew. Chem., Int. Ed.* **2010**, *49*, 1736–1758.
- (3) Recent examples of metal-substituted POMs: (a) Kamata, K.; Yonehara, K.; Nakagawa, Y.; Uehara, K.; Mizuno, N. *Nat. Chem.* **2010**, *2*, 478–483. (b) Kikukawa, Y.; Yamaguchi, K.; Mizuno, N. *Angew. Chem., Int. Ed.* **2010**, *49*, 6096–6100. (c) Mitchell, S. G.; Molina, P. L.; Khanra, S.; Miras, H. N.; Prescimone, A.; Cooper, G. J. T.; Winter, R. S.; Brechin, E. K.; Long, D.-L.; Cogdell, R. J.; Cronin, L. *Angew. Chem., Int. Ed.* **2011**, *50*, 9154–9157. (d) Suzuki, K.; Kikukawa, Y.; Uchida, S.; Tokoro, H.; Imoto, K.; Ohkoshi, S.; Mizuno, N. *Angew. Chem., Int. Ed.* **2012**, *51*, 1597–1612. (e) Kikukawa, Y.; Kuroda, K.; Yamaguchi, K.; Mizuno, N. *Angew. Chem., Int. Ed.* **2012**, *51*, 2434–2437. (f) Ritchie, C.; Ferguson, A.; Nojiri, H.; Miras, H. N.; Song, Y.-F.; Long, D.-L.; Burkholder, E.; Murrie, M.; Koegerler, P.; Brechin, E. K.; Cronin, L. *Angew. Chem., Int. Ed.* **2008**, *47*, 5609–5612. (g) Compain, J.-D.; Mialane, P.; Dolbecq, A.; Mbomekalle, I. M.; Marrot, J.; Secheresse, F.; Riviere, E.; Rogez, G.; Wernsdorfer, W. *Angew. Chem., Int. Ed.* **2009**, *48*, 3077–3081. (h) Ibrahim, M.; Lan, Y.; Bassil, B. S.; Xiang, Y.; Suchopar, A.; Powell, A. K.; Kortz, U. *Angew. Chem., Int. Ed.* **2011**, *50*, 4708–4711.
- (4) (a) Boglio, C.; Micoine, K.; Rémy, P.; Hasenknopf, B.; Thorimbert, S.; Lacôte, E.; Malacria, M.; Afonso, C.; Tabet, J.-C. *Chem.—Eur. J.* **2007**, *13*, 5426–5432. (b) Kikukawa, Y.; Yamaguchi, S.; Tsuchida, K.; Nakagawa, Y.; Uehara, K.; Yamaguchi, K.; Mizuno, N. *J. Am. Chem. Soc.* **2008**, *130*, 5472–5478. (c) Kikukawa, Y.; Yamaguchi, S.; Nakagawa, Y.; Uehara, K.; Uchida, S.; Yamaguchi, K.; Mizuno, N. *J. Am. Chem. Soc.* **2008**, *130*, 15872–15878. (d) Bosco, M.; Rat, S.; Dupré, N.; Hasenknopf, B.; Lacôte, E.; Malacria, M.; Rémy, P.

Kovensky, J.; Thorimbert, S.; Wadouachi, A. *ChemSusChem* **2010**, *3*, 1249–1252.

- (5) (a) Peacock, R. D.; Weakley, T. J. R. *J. Chem. Soc. A* **1971**, 1836–1839. (b) Kim, K.-C.; Pope, M. T.; Gama, G. J.; Dickman, M. H. *J. Am. Chem. Soc.* **1999**, *121*, 11164–11170. (c) Sadakane, M.; Dickman, M. H.; Pope, M. T. *Angew. Chem., Int. Ed.* **2000**, *39*, 2914–2916. (d) Howell, R. C.; Perez, F. G.; Jain, S.; Horrocks, W. DeW., Jr.; Rheingold, A. L.; Francesconi, L. C. *Angew. Chem., Int. Ed.* **2001**, *40*, 4031–4034. (e) Naruke, H.; Yamase, T. *Bull. Chem. Soc. Jpn.* **2002**, *75*, 1275–1282. (f) Fang, X.; Anderson, T.; Neiwert, W. A.; Hill, C. L. *Inorg. Chem.* **2003**, *42*, 8600–8602. (g) Fang, X.; Anderson, T. M.; Benelli, C.; Hill, C. L. *Chem.—Eur. J.* **2005**, *11*, 712–718. (h) Mialane, P.; Dolbecq, A.; Sécheresse, F. *Chem. Commun. (Cambridge, U. K.)* **2006**, 3477–3485. (i) Bassil, B. S.; Dickman, M. H.; Kammer, B.; Kortz, U. *Inorg. Chem.* **2007**, *46*, 2452–2458. (j) Barsukova, M.; Dickman, M. H.; Visser, E.; Mal, S. S.; Kortz, U. *Z. Anorg. Allg. Chem.* **2008**, *634*, 2423–2427. (k) Khoshnavazi, R.; Sadeghi, R.; Bahrami, L. *Polyhedron* **2008**, *27*, 1855–1859. (l) Ibrahim, M.; Mal, S. S.; Bassil, B. S.; Banerjee, A.; Kortz, U. *Inorg. Chem.* **2011**, *50*, 956–960. (m) Villanneau, R.; Racimor, D.; Messner-Henning, E.; Rousselière, H.; Picart, S.; Thouvenot, R.; Proust, A. *Inorg. Chem.* **2011**, *50*, 1164–1166. (n) Li, Y. G.; Xu, L.; Gao, G. G.; Jiang, N.; Liu, H.; Li, F. Y.; Yang, Y. Y. *CrystEngComm* **2009**, *11*, 1512–1514. (o) Khoshnavazi, R.; Bahrami, L.; Gholamyan, S. *J. Mol. Struct.* **2011**, *990*, 57–62. (p) Zhang, S.; Wang, Y.; Zhao, J.; Ma, P.; Wang, J.; Niu, J. *Dalton Trans.* **2012**, *41*, 3764–3772.

- (6) (a) Bassil, B. S.; Dickman, M. H.; Römer, I.; Kammer, B.; Kortz, U. *Angew. Chem., Int. Ed.* **2007**, *46*, 6192–6195. (b) Hussain, F.; Conrad, F.; Patzke, G. R. *Angew. Chem., Int. Ed.* **2009**, *48*, 9088–9091. (c) Reinoso, S.; Giménez-Marqués, M.; Galán-Mascarós, J. R.; Vitoria, P.; Gutiérrez-Zorrilla, J. M. *Angew. Chem., Int. Ed.* **2010**, *49*, 8384–8388.

- (7) Lewis acid catalysis of RE-containing POMs: (a) Boglio, C.; Lemiére, G.; Hasenknopf, B.; Thorimbert, S.; Lacôte, E.; Malacria, M. *Angew. Chem., Int. Ed.* **2006**, *45*, 3324–3327. (b) Dupré, N.; Rémy, P.; Micoine, K.; Boglio, C.; Thorimbert, S.; Lacôte, E.; Hasenknopf, B.; Malacria, M. *Chem.—Eur. J.* **2010**, *16*, 7256–7264. (c) Moll, H. E.; Nohra, B.; Mialane, P.; Marrot, J.; Dupré, N.; Riflade, B.; Malacria, M.; Thorimbert, S.; Hasenknopf, B.; Lacôte, E.; Aparicio, P. A.; López, X.; Poblet, J. M.; Dolbecq, A. *Chem.—Eur. J.* **2011**, *17*, 14129–14138.

- (8) Ogasawara, Y.; Itagaki, S.; Yamaguchi, K.; Mizuno, N. *ChemSusChem* **2011**, *4*, 519–525.

(9) We have reported that POMs with large negative charges can act as nucleophilic (base) catalysts.¹⁰ For example, (TMS)CN can be nucleophilically activated by $[\gamma\text{-SiW}_{10}\text{O}_{36}]^{8-}$, followed by the reaction with water to form trimethylsilanol.

- (10) Kikukawa, Y.; Suzuki, K.; Sugawa, M.; Hirano, T.; Kamata, K.; Yamaguchi, K.; Mizuno, N. *Angew. Chem., Int. Ed.* **2012**, *51*, 3686–3690.

- (11) Brown, I. D.; Altermatt, D. *Acta Crystallogr.* **1985**, *B41*, 244–247.

- (12) (a) Xin, H.; Li, Y.; Shi, M.; Bian, Z. Q.; Huang, C. H. *J. Am. Chem. Soc.* **2003**, *125*, 7166–7167. (b) Petit, S.; Baril-Robert, F.; Pilet, G.; Reber, C.; Luneau, D. *Dalton Trans.* **2009**, 6809–6815. (c) Sun, M.-L.; Zhang, J.; Lin, Q.-P.; Yin, P.-X.; Yao, Y.-G. *Inorg. Chem.* **2010**, *49*, 9257–9264.

- (13) Pimentel, G. C.; McClellan, A. L. *The Hydrogen Bond*; W. H. Freeman: San Francisco, CA, USA, 1960.

- (14) Shannon, R. D. *Acta Crystallogr.* **1976**, *A32*, 751–767.

- (15) The IR spectra of TBA₆RE-POM in other frequency regions were almost identical (Figure S3) among these compounds because they are essentially isostructural in the anion parts (Figure S1).

(16) Although the complete structural determination of TBA₆Nd-POM has been unsuccessful by X-ray crystallographic analysis because of the severe disorder around the neodymium cations and TBA molecules, the X-ray crystallographic analysis showed that the structure of TBA₆Nd-POM was almost identical to that of TBA₆Nd-POM. The results of IR, CSI-MS, elemental analysis, and crystallo-

graphic data showed that the difference between TBA₈Nd-POM and TBA₉Nd-POM was the numbers of TBA cations.

(17) The CSI-MS of the mixture of TBA₈Nd-POM and 30 equiv of (TMS)CN in 1,2-dichloroethane showed sets of signals centered at m/z 7528, 7448, 7357, 3886, 3845, and 3800 assignable to [TBA₉(TMS)₂CNHNd₂(SiW₁₀O₃₆)₂]⁺, [TBA₉(TMS)HNd₂(SiW₁₀O₃₆)₂(H₂O)]⁺, [TBA₉H₂Nd₂(SiW₁₀O₃₆)₂]⁺, [TBA₁₀(TMS)₂CNHNd₂(SiW₁₀O₃₆)₂]²⁺, [TBA₁₀(TMS)HNd₂(SiW₁₀O₃₆)₂(H₂O)]²⁺, and [TBA₁₀H₂Nd₂(SiW₁₀O₃₆)₂]²⁺, respectively, indicating that TMS cations surrounded the POM anions (Figure S10).

(18) Homogeneously catalyzed cyanosilylation: (a) Park, B. Y.; Ryu, K. Y.; Park, J. H.; Lee, S.-g. *Green Chem.* **2009**, *11*, 946–948. (b) Kuroono, N.; Yamaguchi, M.; Suzuki, K.; Ohkuma, T. *J. Org. Chem.* **2005**, *70*, 6530–6532. (c) Bandini, M.; Cozzi, P. G.; Garelli, A.; Melchiorre, P.; Umani-Ronchi, A. *Eur. J. Org. Chem.* **2002**, 3243–3249. (d) Saravanan, P.; Anand, R. V.; Singh, V. K. *Tetrahedron Lett.* **1998**, *39*, 3823–3824. (e) Yang, Y.; Wang, D. *Synlett* **1997**, 1379–1380. (f) Whitesell, J. K.; Apodaca, R. *Tetrahedron Lett.* **1996**, *37*, 2525–2528. (g) Matsubara, S.; Takai, T.; Utimoto, K. *Chem. Lett.* **1991**, 1447–1450. (h) Kobayashi, S.; Tsuchiya, Y.; Mukaiyama, T. *Chem. Lett.* **1991**, 537–540. (i) Noyori, R.; Murata, S.; Suzuki, M. *Tetrahedron* **1981**, *37*, 3899–3910.

(19) Heterogeneously catalyzed cyanosilylation: (a) Ogasawara, Y.; Uchida, S.; Yamaguchi, K.; Mizuno, N. *Chem.—Eur. J.* **2009**, *15*, 4343–4349. (b) Procopio, A.; Das, G.; Nardi, M.; Oliverio, M.; Pasqua, L. *ChemSusChem* **2008**, *1*, 916–919. (c) Iwanami, K.; Choi, J.-C.; Lu, B.; Sakakura, T.; Yasuda, H. *Chem. Commun. (Cambridge, U. K.)* **2008**, 1002–1004. (d) Cho, W. K.; Lee, J. K.; Kang, S. M.; Chi, Y. S.; Lee, H.-S.; Chio, I. S. *Chem.—Eur. J.* **2007**, *13*, 6351–6358. (e) Huh, S.; Chen, H.-T.; Wiench, J. W.; Pruski, M.; Lin, V. S.-Y. *Angew. Chem., Int. Ed.* **2005**, *44*, 1826–1830. (f) Yamaguchi, K.; Imago, T.; Ogasawara, Y.; Kasai, J.; Kotani, M.; Mizuno, N. *Adv. Synth. Catal.* **2006**, *348*, 1516–1520. (g) Karimi, B.; Ma'Mani, L. *Org. Lett.* **2004**, *6*, 4813–4815. (h) Higuchi, K.; Onaka, M.; Izumi, Y. *Bull. Chem. Soc. Jpn.* **1993**, *66*, 2016–2032.

(20) Asymmetric cyanosilylation: (a) Khan, N. H.; Kureshy, R. I.; Abdi, S. H. R.; Agrawal, S.; Jasra, R. V. *Coord. Chem. Rev.* **2008**, *252*, 593–623. (b) Shen, Y.; Feng, X.; Li, Y.; Zhang, G.; Jiang, Y. *J. Org. Chem.* **2004**, 129–137. (c) Deng, H.; Isler, M. P.; Snapper, M. L.; Hoveyda, A. H. *Angew. Chem., Int. Ed.* **2002**, *41*, 1009–1012. (d) Evans, O. R.; Ngo, H. L.; Lin, W. J. *Am. Chem. Soc.* **2001**, *123*, 10395–10396. (e) Hamashima, Y.; Sawada, D.; Kanai, M.; Shibasaki, M. *J. Am. Chem. Soc.* **1999**, *121*, 2641–2642. (f) Zhang, Z.; Lippert, K. M.; Hausmann, H.; Kotke, M.; Schreiner, P. R. *J. Org. Chem.* **2011**, *76*, 9764–9776. (g) Lv, C.; Cheng, Q.; Xu, D.; Wang, S.; Xia, C.; Sun, W. *Eur. J. Org. Chem.* **2011**, 3407–3411. (h) Dang, D.; Wu, P.; He, C.; Xie, Z.; Duan, C. *J. Am. Chem. Soc.* **2010**, *132*, 14321–14323. (i) Belokon, Y. N.; Caveda-Cepas, S.; Green, B.; Ikonnikov, N. S.; Khrustalev, V. N.; Larichev, V. S.; Moskalenko, M. A.; North, M.; Orizu, C.; Tararov, V. I.; Tasinazzo, M.; Timofeeva, G. I.; Yashkina, L. V. *J. Am. Chem. Soc.* **1999**, *121*, 3968–3973. (j) Kuroono, N.; Arai, K.; Uemura, M.; Ohkuma, T. *Angew. Chem., Int. Ed.* **2008**, *47*, 6643–6646. (k) Zhang, Z.; Wang, Z.; Zhang, R.; Ding, K. *Angew. Chem., Int. Ed.* **2010**, *49*, 6746–6750.

(21) (a) Kamata, K.; Yonehara, K.; Sumida, Y.; Yamaguchi, K.; Hikichi, S.; Mizuno, N. *Science* **2003**, *300*, 964–966. (b) Kamata, K.; Kotani, M.; Yamaguchi, K.; Hikichi, S.; Mizuno, N. *Chem.—Eur. J.* **2007**, *13*, 639–648.

(22) (a) *CrystalClear* 1.3.6; Rigaku and Rigaku/MS: The Woodlands, TX, USA (b) Pflugrath, J. W. *Acta Crystallogr.* **1999**, *D55*, 1718–1725.

(23) Otwinowski, Z.; Minor, W. Processing of X-ray Diffraction Data Collected in Oscillation Mode. In *Methods Enzymology*; Carter, C. W., Jr., Sweet, R. M., Eds.; Macromolecular Crystallography, Part A; Academic Press: New York, 1997; Vol. 276, pp 307–326.

(24) *CrystalStructure* 3.8; Rigaku and Rigaku/MS: The Woodlands, TX, USA.

(25) Farrugia, L. J. *J. Appl. Crystallogr.* **1999**, *32*, 837–838.

(26) Yadokari-XG, Software for Crystal Structure Analyses, Wakita K. 2001; Release of Software (Yadokari-XG 2009) for Crystal Structure Analyses: Kabuto, C.; Akine, S.; Nemoto, T.; Kwon, E. *J. Cryst. Soc. Jpn.* **2009**, *51*, 218–224.

(27) Sheldrick, G. M. *SHELX97, Programs for Crystal Structure Analysis*, Release 97-2; University of Göttingen: Göttingen, Germany, 1997.